Catalysis Letters 44 (1997) 75–81

Non-Faradaic catalysis: the case of CO oxidation over Ag–Pd alloy electrode in a solid oxide electrolyte cell

T.I. Politova, V.V. Gal'vita, V.D. Belyaev and V.A. Sobyanin*

Federal Research Center "Boreskov Institute of Catalysis", Novosibirsk 630090, Russia
E-mail: sobyanin@catalysis.nsk.su

Received 17 May 1996; accepted 9 December 1996

Studies of carbon monoxide oxidation on an Ag–25 at% Pd alloy electrode in a cell with a solid oxygen-conducting electrolyte – $CO + O_2$, Ag–Pd | $0.9ZrO_2 + 0.1Y_2O_3$ | $Pt + PrO_{2-x}$, air – were carried out. XRD, SEM and XPS techniques were used for characterisation of the Ag–Pd alloy electrode. The non-Faradaic effect of electrochemical oxygen pumping on the rate of carbon monoxide oxidation was demonstrated. The induced change in the reaction rate at cathodic polarization of the Ag–Pd alloy electrode was an order of magnitude higher than the rate of oxygen pumping from the reaction zone through the electrolyte. The observed phenomenon was qualitatively explained on the base of a chain reaction mechanism involving electrochemically generated oxygen species.

Keywords: carbon monoxide oxidation, silver–palladium alloy, solid oxide electrolyte cell, NEMCA phenomenon

1. Introduction

Recently much attention has been paid [1–3] to the study of oxidative conversion of gases (CO, CH_4, C_2H_4, CH_3OH) over metal electrode-catalysts in a solid oxygen-conducting electrolyte cell:

$$\text{gas} + O_2, \text{metal catalyst} \mid ZrO_2\ (8-10\ \text{mol\%}\ Y_2O_3) \mid \text{metal}, O_2\,.$$

The current passing through the cell (a flow of O^{2-} ions through the electrolyte) was found to change remarkably and reversibly the activity of the metal catalyst. The induced change in the catalytic rate exceeded by several orders of magnitude the rate of oxygen flow through the electrolyte. This novel effect has been termed non-Faradaic electrochemical modification of catalytic activity (NEMCA effect).

The NEMCA effect has been already studied for more than 30 catalytic systems and it is a general phenomenon [1–3]. This effect was demonstrated for carbon monoxide oxidation on Pd [2], Ag [3], Pt [4], and Au [5] electrodes.

The present paper is devoted to investigation of the influence of electrochemical oxygen pumping on CO oxidation over the Ag–25 at% Pd alloy electrode-catalyst in the cell with a solid oxygen-conducting electrolyte:

$$CO + O_2, \text{Ag–Pd} \mid ZrO_2\ (10\ \ \text{mol\%}\ Y_2O_3) \mid Pt + PrO_{2-x}, \text{air}\,.$$

Electrochemical properties of Ag–Pd alloys deposited on a solid oxygen-conducting electrolyte were studied in oxygen atmosphere in detail [6,7]. It was found that silver-rich alloys are stable to oxidation; they are active electrodes for electrochemical oxidation and reduction of oxygen. However, little is known as yet about the catalytic properties of Ag–Pd alloy with respect to the CO oxidation. We are aware of only three works [8–10]. The authors of refs. [8,9] no more than mention that a freshly prepared Ag–Pd alloy is highly active, but its activity decreases crucially in time. Only the activation energy of the reaction was measured in ref. [10].

2. Experimental

The electrochemical cell was a tube closed at one end made of yttria-stabilised zirconia (YSZ) electrolyte. The electrolyte tube was 150 mm in length, 10 mm in diameter and had 0.6 mm wall thickness. An Ag–25 at% Pd (working) electrode was deposited on the outer surface of the zirconia tube. A quartz jacket, equipped with gas supply lines, covered the tube. The reaction mixture was fed to the annulus space between the quartz jacket and zirconia tube. A Pt electrode containing praseodymium oxide was deposited on the inner surface of the zirconia tube and served as counter and reference electrode simultaneously. The Pt electrode was blown with air. The geometrical area of Ag–Pd and Pt electrodes was 3 cm^2. There were ca. 5–7 mg/cm^2 Pt and Ag–Pd alloy loadings in an electrode.

The principle of the experiments was as follows. With an open circuit in the cell, a typical heterogeneous catalytic reaction of CO oxidation takes place on the Ag–Pd electrode-catalyst. Upon passing current through the cell the electrode-catalyst can be, depending on the polarity of the applied current, either anode or

---

* To whom correspondence should be addressed.

cathode, which results in oxygen pumping to or from the reaction zone through the electrolyte. The effect of electrochemical pumping of oxygen on the CO oxidation rate was the subject for study.

The effect of current on the rate of catalytic reaction over the electrode deposited on YSZ is described [1–3] by two dimensionless parameters: $\rho = r/r_0$ and $\Lambda = (r - r_0)/(I/4F)$, where r_0 and r are rates of the catalytic reaction (g-atom O/s) under open- and closed-circuit conditions, respectively; I is the current passing through the cell; F is Faraday's constant. Rate enhancement ratio ρ shows the reaction rate variation affected by the current with respect to the rate upon cell circuit opening. Enhancement factor Λ reflects the change in the reaction rate $(r - r_0)$ relative to the oxygen flow rate through the electrolyte $(I/4F)$. Systems exhibiting non-Faradaic catalysis or NEMCA effect are characterised by $\rho \neq 0$ and $|\Lambda| \gg 1$ values.

The electric current flowing through the cell and applied voltage were controlled by a potentiostat–galvanostat. The compositions of the inlet and outlet reaction mixtures were analysed by gas-chromatography. The techniques used for the electrochemical and kinetic measurements have been described in detail elsewhere [11].

The CO oxidation reaction was studied with reaction mixtures rich in oxygen at atmospheric pressure and temperatures of 400–500°C. The inlet concentrations of CO and O_2 were varied in the ranges of 2–8 vol% and 20–75 vol%, respectively. A flow of carbon monoxide, oxygen and inert gas was fed to the Ag–Pd electrode-catalyst at 1 cm^3/s. In a blank test without deposition of Ag–Pd electrode-catalyst on the YSZ tube, the rate of CO oxidation was negligible.

The Ag–25 at% Pd alloy electrode-catalyst was prepared via calcining a paste, containing the desirable quantity of Ag and Pd powders, painted on the surface of the YSZ tube, in air at 900°C for 1.5 h. The electrode characterisation was performed by XRD, SEM and XPS techniques.

X-ray diffraction patterns were recorded using a URD-63 diffractometer with graphite-filtered Cu Kα (1.5406 Å) radiation. Silicon was used as an internal standard. Spectra were recorded with a 2θ scan from 20 to 150° at an angular speed of 0.25° (2θ)/min.

SEM measurements were made with a Tesla BS-350 high-resolution scanning field emission electron microscope.

XPS measurements were carried out with a VG ESCA-3 spectrometer fitted with a sample preparation chamber. Mg Kα (1486.6 eV) radiation was employed for the study.

3. Results

Before discussing the results, let us pay attention to the fact that the rate of CO oxidation and current–voltage characteristics (CVC) of the Ag–Pd alloy electrode were unstable in time during the first experiments. CVC and catalytic activity of the electrode became stable not earlier than after alternate anodic and cathodic polarization of the electrode in the reaction medium applied for ~ 40 h. All the electrochemical and catalytic data discussed here were obtained with the electrode having undergone such a pretreatment.

3.1. XRD, SEM, and XPS

XRD, SEM, and XPS techniques were used to characterise a freshly prepared Ag–Pd alloy electrode (sample 1) and the electrode taken after finishing all the experiments (sample 2).

Similar XRD spectra were recorded for samples 1 and 2. They showed a single-phase Ag–Pd alloy. All peaks could be indexed on the basis of a face-centered cell with lattice constant $a_0 = 4.0374 \pm 0.0003$ Å. This value of a_0 is in agreement with other experimental data for Ag–25 at% Pd [12,13].

The surface composition and the state of the Ag–Pd alloy electrode treated in gas atmospheres of various compositions were examined using XPS. To carry out this study, sample 2 to be treated was placed in the sample preparation chamber. Then the sample was moved to an analytical chamber to record its XP spectrum. The results obtained are summarised in table 1.

Practically no change in the surface alloy composition was observed after different treatment procedures. The surface Pd/Ag atomic ratio is ~0.25–0.27, that is lower than the bulk ratio (Pd/Ag $\approx$ 0.33). Enriching of the alloy surface with silver is a well known phenomenon [14].

The binding energy (BE) of Ag $3d_{5/2}$ is not affected by pretreatments and coincides with the bulk metal value [15]. The Pd $3d_{5/2}$ spectra recorded after pretreatments 1 and 2 (table 1) show no change in BE with respect to the bulk metal value [15]. A shift of BE (Pd $3d_{5/2}$) by ~ 0.3 eV appeared only after pretreatment with oxygen, that is, probably, caused by adsorption of oxygen. Note that the formation of palladium oxide would result in the shift of the Pd $3d_{5/2}$ line by more than 1 eV [15].

The XRD and XPS data obtained allow the assumption that the Ag–25 at% Pd alloy electrode is resistant to oxidation and to "de-alloying" under the experimental conditions of this work. This conclusion is in agreement with literature data reported for a silver-rich Ag–Pd alloy (the alloy studied in this work belongs to this type too). In particular, it was shown in refs. [6,7] that a silver-rich alloy electrode deposited on YSZ, unlike a palladium-rich alloy, is resistant to oxidation by oxygen and stable at anodic polarization of the electrode. Moreover, in contrast to the palladium-rich Ag–Pd alloy, the silver-rich alloy used to catalyse ethylene oxidation was found to have the same lattice constant as the bulk material [16].

Table 1
XPS data on Ag–Pd alloy electrode (sample 2)

Pretreatment	Binding energy (eV)		Pd/Ag atomic ratio
	Pd $3d_{5/2}$	Ag $3d_{5/2}$	
(1) Ar^+-ion etching and annealing in vacuum. $T = 500°C$, $\tau = 2$ h	335.2	368.3	0.25
(2) 1 + annealing in reaction mixture. $T = 400–500°C$, $P = 50$ Torr, $O_2/CO = 4$, $\tau = 2$ h	335.1	368.3	0.27
(3) 1 + 2 + annealing in oxygen. $T = 400–500°C$, $P = 50$ Torr, $\tau = 2$ h	335.5	368.3	0.26

The Ag–Pd alloy electrode structure was examined by SEM. SEM micrographs of samples 1 and 2 are presented in fig. 1. "By eye" comparison evidences for the significant difference between the structure of the freshly prepared electrode (figs. 1a, 1c, 1e) and the structure of the spent electrode (figs. 1b, 1d, 1f). The freshly prepared electrode (sample 1) is a ~ 5 μm thick film being in a good contact with YSZ (fig. 1a). The film consists of a tight ensemble of small-sized crystallites (figs. 1c and 1e).

The spent electrode (sample 2) is a thicker film (~ 10–12 μm) being in good contact with YSZ too (fig. 1b). The film is constituted by larger crystallites (fig. 1f) and possesses a fine structure involving a ramified system of macropores of 1–30 μm in size (fig. 1d).

Thus, although the Ag–Pd alloy electrode is stable to oxidation and "de-alloying", its structure changes significantly in the course of its working. Probably, the electrode structure rearrangement bears responsibility for unstable CVC and changeable activity of the alloy during the starting experiments. After all, the electrode structure is stabilized as sample 2, CVC and the catalytic activity become reproducible.

3.2. CO oxidation under open-circuit conditions

When $CO–O_2$ reaction mixtures rich in oxygen ($[O_2]/[CO] = 4–12$) are fed through the cell, the open-circuit potential takes the values of between −40 and −10 mV. This indicates that oxygen activity (a) on the electrode-catalyst, determined from refs. [2,3] as

$$a = (0.21)^{1/2} \exp(2FE/RT) ,$$

is lower than the gas-phase oxygen activity $a_0 = P_{O_2}^{1/2}$, where P_{O_2} is the oxygen pressure. Thus oxygen adsorbed on Ag–Pd alloy surface is not in equilibrium with the gaseous oxygen under the reaction conditions. The same result was obtained for CO oxidation on the Pt [4] and Au [5] electrodes.

Effects of temperature and the concentration of reagents on the rate of CO oxidation were studied. It was found that at a temperature range from 350 to 500°C an apparent activation energy of the reaction is 4 ± 1 kcal/mol. This value disagrees with the activation energy of 11.6 kcal/mol determined in ref. [10]. The discrepancy in the activation energy may be due to the different compositions of the alloys (Ag–25 at% Pd and Ag–5 at% Pd) and reaction mixtures ($[O_2]/[CO] \approx 5$ and ≈ 0.25) used in the present study and in ref. [10].

Fig. 2 shows the effect of concentration of reagents on the rate of CO oxidation. It can be seen that the rate of CO_2 formation is first order in carbon monoxide and zero order in oxygen. It should be noted that the observed concentration dependencies of the rate are typical for CO oxidation on metals with reaction mixture rich in oxygen.

The observed kinetic data permit us to make some conclusions about the mechanism of CO oxidation on Ag–Pd alloy. It seems reasonable to suppose that the reaction follows the Eley–Rideal mechanism involving the atomic oxygen state Z_0O, whose surface coverage is close to unit:

$$O_2 + 2Z_0 \rightarrow 2Z_0O$$

$$Z_0O + CO \rightarrow CO_2$$

In this case the reaction orders in CO and O_2 should be equal to 1 and 0, respectively, which is in agreement with experimental data.

The Langmuir–Hinshelwood mechanism can also be proposed. For example, a weakly bound molecular state of CO can take part in the process too.

3.3. CO oxidation under closed-cicuit conditions

Fig. 3 shows the galvanostatic transient rate of CO_2 formation and IR-free electrode potential at CO oxidation on Ag–Pd alloy electrode upon applying cathodic ($I = -2.4$ mA) and anodic ($I = 5.1$ mA) currents. One can see that the cathodic and anodic currents lead to a change in the electrode potential and to a non-Faradaic enhancement of the reaction rate. Upon applying the cathodic current the ratio ρ and the factor Λ were 3.7 and 30, respectively. Upon applying the anodic current ρ and Λ values were 1.4 and 2, respectively. After the current passing through the cell had been turned off, the reaction rate and electrode potential returned to their open-circuit values. Turning the current on again resulted in the same phenomena as just discussed. Therefore, there is a reversible effect of current on the electrode potential and the reaction rate.

Figs. 4 and 5 show examples of the effect of current passing through the cell on the CO_2 formation rate dur-

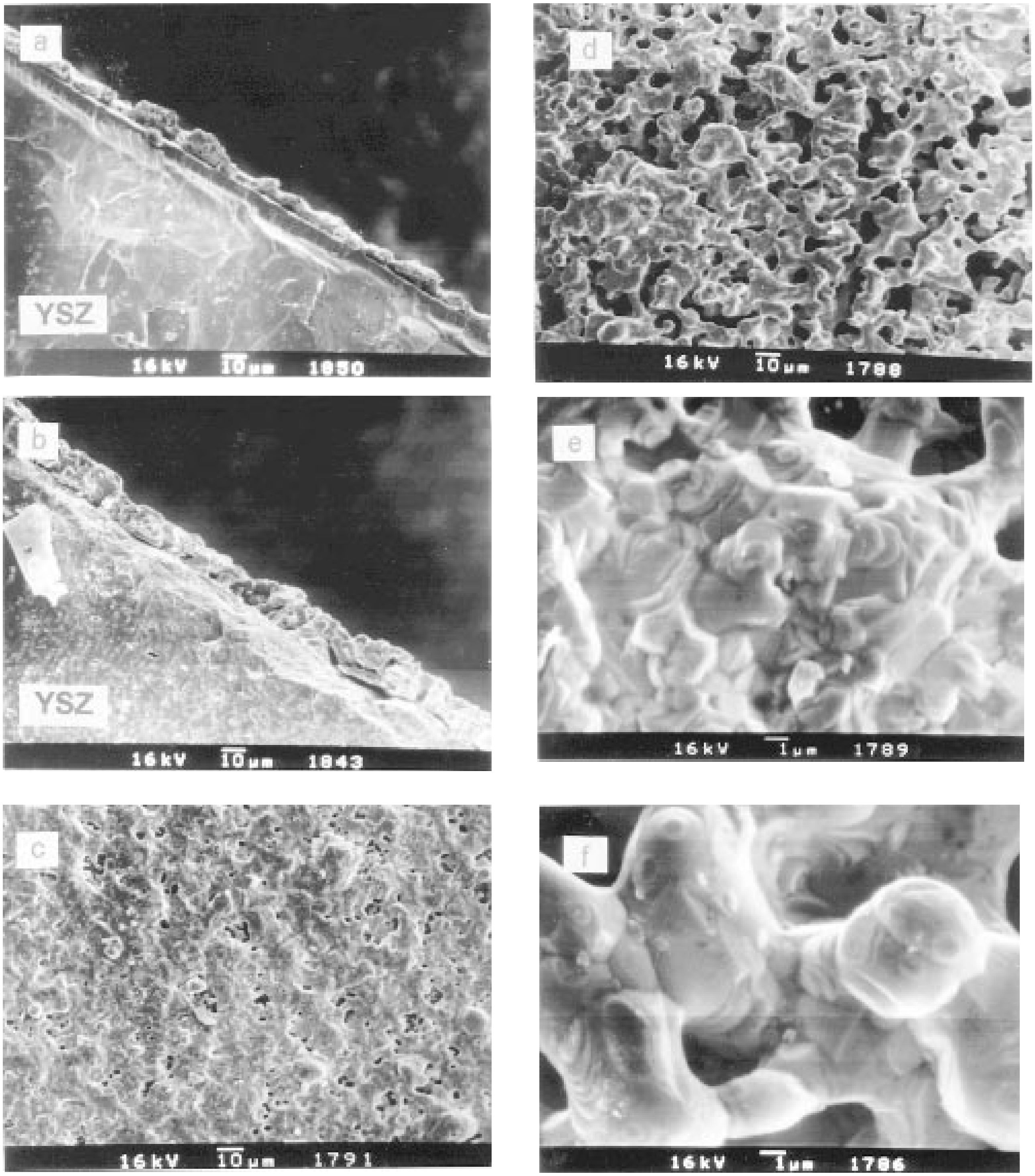

Fig. 1. Scanning electron micrographs of an Ag–25 at% Pd alloy electrode. (a, c, e) sample 1; (b, d, f) sample 2.

ing CO oxidation at 450°C ($[O_2]/[CO] \approx 3.7$) and at 500°C ($[O_2]/[CO] = 5$). All results reported here were obtained under galvanostatic mode of cell operation and after the achievement of steady-state values for electrode potential and reaction rate. It is seen that cathodic ($I < 0$) and anodic ($I > 0$) polarization of Ag–Pd alloy electrode enhance the reaction rates (r) with respect to their open circuit value (r_0) at both 450 (fig. 4) and 500°C (fig. 5). A sharp enhancement of r is observed upon an increase in the cathodic current. Let us discuss these data in detail.

Anodic polarization of Ag–Pd alloy electrode, i.e. oxygen pumping to the catalyst, leads to a slight increase in the reaction rate. Analysis of the data obtained (figs. 4 and 5) has shown that ratio ρ is less then 1.5. Enhancement factor Λ decreases from 3 to 1 with an

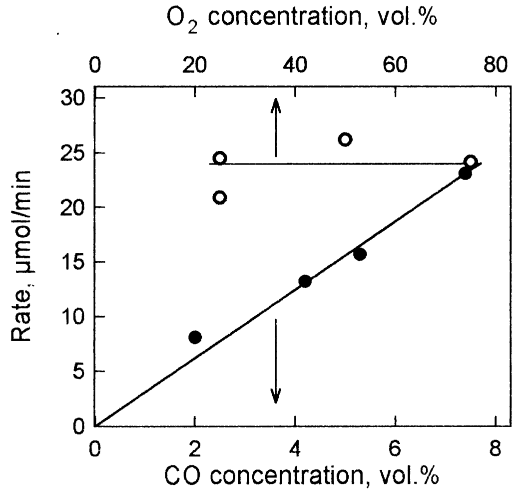

Fig. 2. Effect of gaseous compositions on the rate of CO_2 formation under open-circuit conditions at $T = 450°C$. (●) $[O_2] = 25$ vol%, (○) $[CO] = 6.7$ vol%.

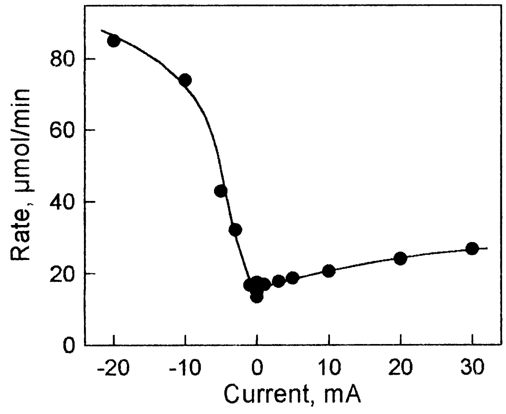

Fig. 4. Effect of applied current on the rate of CO_2 formation. Temperature and inlet composition: $T = 450°C$, $[O_2] = 25$ vol%, $[CO] = 6.5$ vol%.

increase of the applied anodic current. Thus O^{2-} pumping to Ag–Pd electrode at low anodic polarization causes slight non-Faradaic changes in the CO oxidation rate. The current effect on r at high anodic polarization is purely Faradaic.

In recent studies [1–4] it has been found that O^{2-} pumping to Pt, Pd and Ag electrodes enhances dramatically the CO oxidation rate. The results show that $\rho \approx 1.5$–3 and $\Lambda \approx 20$–10^3, i.e., the observed behaviour was non-Faradaic. One might expect that O^{2-} pumping to the Ag–Pd electrode as well as to Pt, Pd and Ag be accompanied by dramatic changes in the rate of CO oxidation. However, the catalytic properties of the Ag–Pd electrode did not alter essentially. The same situation was found in the case of an Au electrode [5].

Cathodic polarization of the Ag–Pd alloy electrode, i.e. oxygen pumping from the catalyst, as shown in figs. 4 and 5, leads to the sharp enhancement of the reaction rates with respect to their open-circuit values. The results obtained have shown that ratio ρ and factor $|\Lambda|$ reach values of ~4–5 and ~20, respectively. Thus, oxygen pumping from the electrode-catalyst was found to cause a non-Faradaic change in the CO oxidation rate.

The same cathodic current effect on the CO oxidation rate has been demonstrated on Au [5] and Ag [3] electrodes. Contradictory data were reported for the Pt electrode [3,4]. According to ref. [4, see figs. 4 and 5], the cathodic polarization of the Pt electrode show a decrease in the rate of CO oxidation with respect to their open-circuit value. In ref. [3, see fig. 44] the opposite cathodic current effect on the rate was found.

4. Discussion

4.1. The nature of NEMCA

The nature of the NEMCA effect was discussed by

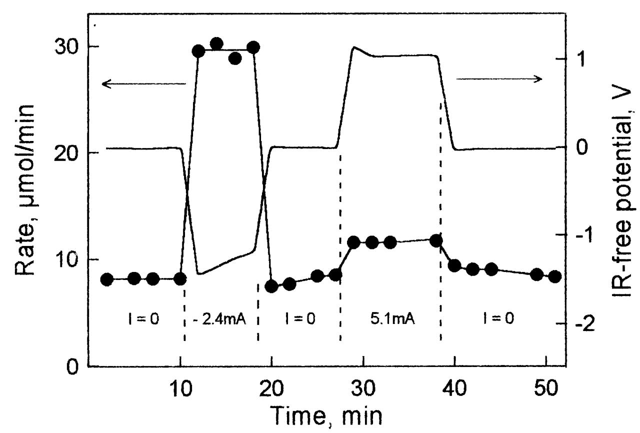

Fig. 3. Transient effect of current on the rate of CO_2 formation and on the electrode-catalyst potential. Temperature and inlet composition: $T = 450°C$, $[O_2] = 25$ vol%, $[CO] = 2$ vol%.

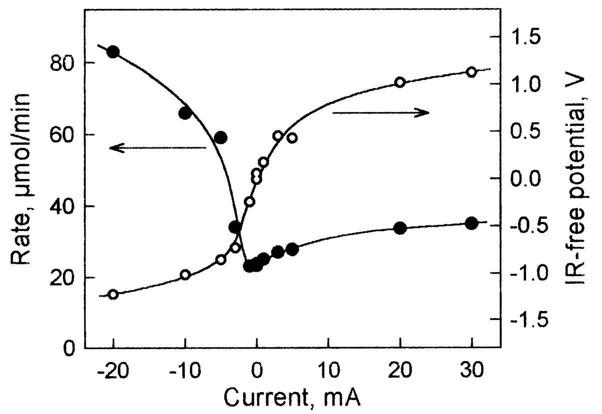

Fig. 5. Effect of applied current on the rate of CO_2 formation and on the IR-free Ag–Pd alloy electrode potential. Temperature and inlet composition: $T = 500°C$, $[O_2] = 25$ vol%, $[CO] = 5$ vol%.

Vayenas et al. in a number of publications [1–3]. According to refs. [1–3] the essence of the NEMCA effect is that the electrode work function changes, during polarization of the metal electrode deposited on the solid oxygen-conducting electrolyte, i.e. when current is passing through the cell. This leads to changes in the strength of the chemisorptive bond of adsorbed oxygen and, hence, in catalytic properties of the electrode for oxidation reactions. We have considered this concept as questionable [5,17] and formulated a chain reaction mechanism involving electrochemically generated oxygen species to explain the NEMCA phenomenon [18].

In particular [18], the non-Faradaic effect of current on the rate of CO oxidation on Pt/YSZ and Au/YSZ electrode-catalysts has been described in terms of this approach. As mentioned before (see section 3.3) there was the same effect of current on the CO_2 formation rate over Ag–Pd/YSZ and Au/YSZ electrodes. The chain mechanism might be also applicable to the case of $CO + O_2$ reaction over Ag–Pd/YSZ electrode. As an example, the simplest mechanism of CO oxidation under NEMCA conditions might be as follows:
(at cathodic polarization of electrode)

$$(1)\ 2Z_0 + O_2 \rightleftharpoons 2Z_0O$$

$$(2)\ Z_0O + CO \rightarrow CO_2 + Z_0$$

$$(3)\ O_2 + Z + 2e \rightarrow 2ZO^- \qquad \text{initiation}$$

$$\left.\begin{array}{l}(4)\ ZO^- + Z_0O \rightarrow ZO_2^- + Z_0 \\ (5)\ ZO_2^- + CO \rightarrow CO_2 + ZO^-\end{array}\right| \quad \text{propagation}$$

$$(6)\ ZO^- + e \rightarrow O^{2-} + Z \qquad \text{termination}$$

(at anodic polarization of electrode)

$$(1')\ 2Z_0 + O_2 \rightleftharpoons 2Z_0O$$

$$(2')\ Z_0O + CO \rightarrow CO_2 + Z_0$$

$$(3')\ O^{2-} + Z \rightarrow ZO^- + e \qquad \text{initiation}$$

$$\left.\begin{array}{l}(4')\ ZO^- + Z_0O \rightarrow ZO_2^- + Z_0 \\ (5')\ ZO_2^- + CO \rightarrow CO_2 + ZO^-\end{array}\right| \quad \text{propagation}$$

$$(6')\ 2ZO^- \rightarrow O_2 + Z + 2e \qquad \text{termination}$$

where Z_0 is a catalytically active site on the gas-exposed surface of the Ag–Pd alloy electrode; Z_0O is atomic oxygen species on the catalytically active site; Z is an electrochemically active site on the three-phase boundary gas/Ag–Pd alloy/YSZ; ZO^- and ZO_2^- are charged oxygen species on the electrochemically active site; O^{2-} is the oxygen anion in the bulk of YSZ.

Steps 1, (1′) and 2, (2′) represent ordinary catalytic reaction following the Eley–Rideal mechanism (see section 3.2). Current-producing steps 3, (3′) and 6, (6′) are chain initiation and chain termination steps, respectively. Their rates are controlled by the current. Steps 4, (4′) and 5, (5′) are chain propagation steps. They are not current-producing steps. Their rates are higher than those of initiation and termination steps.

If so [18], the rate changes under steady-state conditions upon current application can be as large as the chain length ν ($\nu = r_{ch}/(I/4F)$, where r_{ch} is the rate of chain process, when current I is passing through the cell; $I/4F$ is the oxygen flow through the electrolyte or the rate of chain initiation/termination. Evidently, rate changes and ν are determined by the values of rate constants of steps. At present we are carrying out a numerical simulation of the experimental data on CO oxidation under NEMCA conditions for evaluation of the rate constants of the chain mechanism.

Finally, it should be noted that the kinetic scheme is not final and can certainly be modified. In particular, this may concern the nature of electrochemically generated oxygen species; how CO molecules interact with the adsorbed oxygen (e.g. via Eley–Rideal or Langmuir–Hinshelwood mechanisms); and the place where chain propagation steps occur (e.g., on the three-phase boundary gas–electrode–YSZ or on the two-phase boundary gas–electrode). According to our model, only the chain process involving electrochemically generated oxygen species is the key factor for appearance of non-Faradic catalysis.

Acknowledgement

The authors thank INTAS (Project No. 94-3056) and the Russian Foundation of Fundamental Research (Project No. 93-03-5097) for the support of this investigation. They would also like to thank Drs. N.A. Rudina and S.V. Koshcheev for taking the scanning electron micrographs and the XP spectra.

References

[1] C.G. Vayenas, S. Bebelis and S. Ladas, Nature 343 (1990) 625.

[2] C.G. Vayenas, S. Bebelis, I.V. Yentekakis and H.-G. Lintz, Catal. Today 11 (1992) 303.

[3] C.G. Vayenas, M.M. Jaksic, S. Bebelis and S.G. Neophytides, in: *Modern Aspects of Electrochemistry*, No. 29, eds. J.O.M. Bockris et al. (Plenum Press, New York, 1995) pp. 57–202.

[4] V. Yentekakis and C.G. Vayenas, J. Catal. 111 (1988) 170.

[5] O.A. Mar'ina and V.A. Sobyanin, Catal. Lett. 13 (1992) 61.

[6] N.A. Lobovikova and M.V. Perfil'ev, in: *Elektrodnye Protsessi v Galoidnych i Oksidnych Electrolitach*, Sverdlovsk 1981, pp. 91–91, in Russian.

[7] N.A. Lobovikova and M.V. Perfil'ev, in: *Elektrodnye Protsessi v Tverdoelektrolitnych Sistemach*, ed. M.V. Perfil'ev (UrO AN SSSR, Sverdlovsk, 1988) pp. 67–84, in Russian.

[8] V.K. Yatsimirskii, N.A. Boldyreva and T.V. Marchuk, React. Kinet. Catal. Lett. 12 (1979) 339.

[9] V.K. Yatsimirskii, Teoreticheskaja i eksperimental'naja chimija 27 (1991) 574, in Russian.

[10] G.-M. Schwab and K. Gossner, Z. Phys. Chem. NF 16 (1958) 39.

[11] O.A. Mar'ina, V.A. Sobyanin and V.D. Belyaev, Elektrochimija 26 (1990) 1413, in Russian.

[12] B.R. Coles, J. Inst. Metals 84 (1956) 346.

[13] G. Meitzner and J.H. Sinfelt, Catal. Lett. 30 (1995) 1.

[14] V. Ponec, Mater. Sci. Eng. 42 (1980) 135.

[15] C.D. Wagner, W.M. Riggs, L.E. Davis, J.F. Moulder and G.E. Muilenberg, eds., *Handbook of X-ray Photoelectron Spectroscopy* (Perkin-Elmer, Eden Prairie, 1978) p. 190.

[16] R.L. Moss and D.H. Thomas, J. Catal. 8 (1967) 151.

[17] V.A. Sobyanin, V.I. Sobolev, V.D. Belyaev, O.A. Mar'ina, A.K. Demin and A.S. Lipilin, Catal. Lett. 18 (1993) 153.

[18] V.A. Sobyanin and V.D. Belyaev, React. Kinet. Catal. Lett. 51 (1993) 373.